Modelling the law of the wake using an offset from the wall

Grégoire Winckelmans[a)] and Matthieu Duponcheel[b)]

Université catholique de Louvain (UCLouvain), Institute of Mechanics, Materials and Civil Engineering (iMMC), 1348 Louvain-la-Neuve, Belgium

(Dated: 26 May 2021)

We focus on the wake function $F(Y)$, where $Y = y/\delta$: the excess velocity above the logarithmic profile in wall-bounded turbulence. It is first measured using DNS data of turbulent channel flow at $Re_\tau \simeq 5200$, which has a distinguishable overlap layer. The function $Q(Y) = Y\,F'(Y)$ is seen to be significant only beyond $Y_c \simeq 0.16$, and also linear (with a slope $\alpha \simeq 1.15$) up to $Y \simeq 0.5$. Our simplest $Q(Y)$ model is then a linear ramp function that starts at the measured intercept. Our $Q(Y)$ model is furthermore extended up to the channel centre, by subtracting a quadratic term which satisfies the boundary condition at $Y = 1$. The analytical integration of $Q(Y)$ provides the model for the wake function with offset Y_c, and which covers the full range; it is seen to fit very well the DNS data. Our $Q(Y)$ model is also compared to the "extended law of the wall" model without offset. Furthermore, and to comply with some recent literature, a version of our model is also developed with some small slope $\alpha_0 \ll \alpha$ contribution to $Q(Y)$ within the overlap layer. The DNS of a ZPG boundary layer at $Re_\tau \simeq 2300$ is considered next: the amplitude of the wake function is much larger than in channel flow ($\alpha \simeq 7.3$) and the intercept is smaller ($Y_c \simeq 0.11$). The obtained $F(Y)$ model also compares very well with the DNS data over the full range. Lastly, we also revisit Coles wake function model and we show that adding the offset improves it significantly.

[a)]gregoire.winckelmans@uclouvain.be

[b)]matthieu.duponcheel@uclouvain.be

I. INTRODUCTION

The present contribution focuses on the wake function, in an effort for modelling the velocity profile in canonical wall-bounded turbulent flows: channel flow made of two plates separated by a distance $d = 2\,\delta$; zero pressure gradient (ZPG) boundary layer of effective thickness $\delta(x)$; pipe of diameter $D = 2\,\delta$.

The two velocity scales are the global velocity U_0 (centreline velocity U_c in channel and pipe flows; outer velocity U_e in boundary layers) and the wall friction velocity $U_\tau = \sqrt{\tau_w/\rho}$ (with τ_w the wall shear stress and ρ the fluid density). The dimensionless profile is $U^+ = U/U_\tau$. Globally, the distance y to the wall is made dimensionless using δ, and we define $Y = y/\delta$. Close to the wall, y is made dimensionless using the viscous length $l_\nu = \nu/U_\tau$, leading to $y^+ = y/l_\nu = (y\,U_\tau)/\nu$. The friction Reynolds number is $Re_\tau = \delta^+ = (\delta\,U_\tau)/\nu$; hence $Y = y^+/Re_\tau$.

We recall the various regions:

- The "inner region" or "wall layer", for $Y \ll 1$. A strict "law of the wall" (in line with Von Karman[1] and Prandtl[2]) amounts to U^+ being solely a function of y^+ there:

$$U^+ = f(y^+)\ . \tag{1}$$

- The "outer region", for $y^+ \gg 1$, where the "velocity defect" profile is solely a function of Y:

$$U_0^+ - U^+ = D(Y)\ , \tag{2}$$

  which constitutes the "defect law".

- The "overlap layer", which is both "inner" and "outer".

Following the argument by Millikan[3], the simultaneous validity of a strict law of the wall and of the defect law implies that the overlap layer should exhibit a purely logarithmic velocity profile:

$$U^+ = \frac{1}{\kappa}\,\ln(y^+) + C\ , \tag{3}$$

also in line with Von Karman[1] and Prandtl[2].

As we here focus on the overlap layer and beyond, we will write the velocity profile using the composite form of Coles [4]:

$$U^+ = \left(\frac{1}{\kappa}\ \ln(y^+) + C\right) + F(Y) \tag{4}$$

where $F(Y)$ is the "complement function"; also called "wake function" by Coles as its S-shape resembles that of a free shear layer. This is the "law of the wake".

A strict law of the wall thus amounts to having that $F(Y) = 0$ within the overlap layer. Recent modelling obtained using matched asymptotic expansions however allows for $F(Y)$ to have a non-zero, yet moderate, contribution within the overlap layer. We will present below some of the contributions on that point as it relates to our objective: which is to accurately model the wake function (not the discussion on whether or not there a strict law of the wall).

As to the "defect law", it is obtained as:

$$U_0^+ - U^+ = -\frac{1}{\kappa}\ \ln(Y) + (F(1) - F(Y)) = D(Y)\ . \tag{5}$$

Note that the defect law does not require to have a strict law of the wall within the overlap layer: $F(Y)$ can be zero or non-zero there.

As is usual, the profile of the indicator function, $y\,\frac{dU^+}{dy}$, will here be used to investigate, and model, the velocity profile. When focusing on the overlap layer and beyond, as here, one writes:

$$y\,\frac{dU^+}{dy} = \frac{1}{\kappa} + Y\,F'(Y) = \frac{1}{\kappa} + Q(Y) \tag{6}$$

where we have defined the function $Q(Y) = Y\,F'(Y)$; we note that it has a boundary condition: $Q(1) = F'(1) = -\frac{1}{\kappa}$. The proposition that $F(Y)$ already contributes in the overlap layer, and thus that $Q(Y)$ is not strictly zero there, was retained by various authors. Using an asymptotic analysis based on matched asymptotic expansions (with l_ν as inner scale and δ as outer scale), the log law with $B = \frac{1}{\kappa_\infty}$ is obtained as the leading order term. The next term obtained in the expansion should then capture the lowest order finite Reynolds number effects. Such methodology was already applied to moderately large Reynolds number pipe and channel flows by Afzal and Yajnik [5]. Later on, Jiménez and Moser [6] used moderate Reynolds number DNS data of channel flow (Re_τ = 550, 940 and 2000) to fit the proposition,

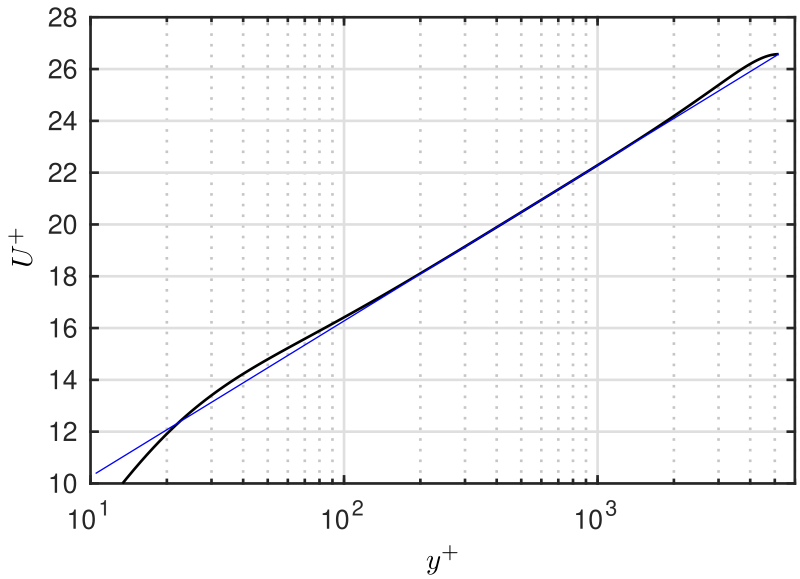

FIG. 1. Channel flow at $Re_\tau \simeq 5200$ - Velocity U^+ (the part $y^+ \leq 10$ is not shown) : DNS[7] (black) and log-law with $\frac{1}{\kappa} = 2.61$ and $C = 4.25$ (blue).

consistent with the matched asymptotic expansion, that

$$y\,\frac{dU^+}{dy} = \left(\frac{1}{\kappa_\infty} + \frac{\gamma}{Re_\tau}\right) + \alpha\,Y + \ldots \quad \Leftrightarrow \quad U^+ = \left(\left(\frac{1}{\kappa_\infty} + \frac{\gamma}{Re_\tau}\right)\,\ln(y^+) + C\right) + \alpha\,Y + \ldots\ , \tag{7}$$

and they proposed $\frac{1}{\kappa_\infty} \simeq 2.49$, $\gamma \simeq 150$ and $\alpha \simeq 1.0$. They however stressed that "these estimates must be considered preliminary, since the overlap layer is marginal at $Re_\tau = 940$". Note that even the case $Re_\tau = 2000$ is marginal.

In Bernardini, Pirozzoli, and Orlandi[8], they also use

$$y\,\frac{dU^+}{dy} = \frac{1}{\kappa} + \alpha\,Y + \ldots \quad \Leftrightarrow \quad U^+ = \left(\frac{1}{\kappa}\,\ln(y^+) + C\right) + \alpha\,Y + \ldots\ , \tag{8}$$

as an "extended law of the wall" profile, and with $\alpha \simeq 1.15$ measured in channel flow. They also argue that this profile is valid up to $Y_r \simeq 0.5$. Our present analysis below will agree with those two values of α and Y_r; yet we will also use the significant offset Y_c.

A similar proposition is found in Luchini[9,10]: he argued that the function $y\,\frac{dU^+}{dy}$ is no longer a constant in the overlap layer, but rather an arbitrary function of the dimensionless pressure gradient $P_x^+ = \frac{1}{\rho}\frac{dp}{dx}/{U_\tau}^2$. Considering that P_x^+ is a small perturbation, the function was taken linear in that perturbation, which led to:

$$y\,\frac{dU^+}{dy} = \frac{1}{\kappa} - \alpha\, P_x^+\, y + \dots \;. \qquad (9)$$

Since $-P_x^+ = \frac{1}{\delta}$ in a channel flow, this corresponds to the same models as above. He also proposed, from the data he investigated, that $\alpha \simeq 1.0$. (He furthermore argued that the correction term would be $2\alpha\, Y$ for pipe flows, as the momentum balance provides $-P_x^+ = \frac{2}{\delta}$.)

Quality channel flow DNS data at a significantly higher Reynolds number of $Re_\tau \simeq 5200$ became available recently, see Lee and Moser [7]. Those data display a sufficiently good separation of scales to make further progress. The velocity profile U^+ is provided in Fig 1, and the function $y\,\frac{dU^+}{dy}$ is provided in Fig. 2. We observe a fair overlap layer, with a "pseudo-plateau" (in blue) in some range: say from $Y \simeq 0.06$ (or $y^+ \simeq 300$, see also Fig. 3) to $Y \simeq 0.16$ (or $y^+ \simeq 800$). We write "pseudo-plateau" as it is slightly tilted.

Lee and Moser [7] also used those data to revisit the numbers previously provided in Jiménez and Moser [6]: most importantly, they modified their view on the term $\alpha\, Y$: it went down significantly: from $\alpha = 1.0$ to only 0.2. In essence, the slight tilt of the pseudo-plateau is indeed that small slope, see Fig. 2 (in green) ; whereas, in all previous investigations mentioned above, and also ours here, the slope of interest is the significant one measured in the region after the pseudo-plateau (in red): that slope is here measured as $\alpha \simeq 1.15$ (i.e., identical to that in Bernardini, Pirozzoli, and Orlandi [8]) and is also shown in Fig. 2. We also see that it remains valid for a significant portion of the channel: up to $Y \simeq 0.5$. **Important notation**: to make a clear distinction in all that follows, we will use α_0 to denote the small slope of the tilt in the overlap layer, and we will keep α to denote the large slope of the line with offset: thus $\alpha_0 \simeq 0.2$ and $\alpha \simeq 1.15$.

It is the large slope α, together with the offset Y_c, that matter the most as far as modelling the wake function $F(Y)$ up to $Y \simeq 0.5$. Our first and simplest model will solely use those, and it will already fit the DNS data very well.

We furthermore note that the offset Y_c is also confirmed when we examine the recent "two state model" by Krug, Philip, and Marusic [11]: with the inertial self-similar region (pure wall flow state with the log law) and the free stream state, with a jump in velocity

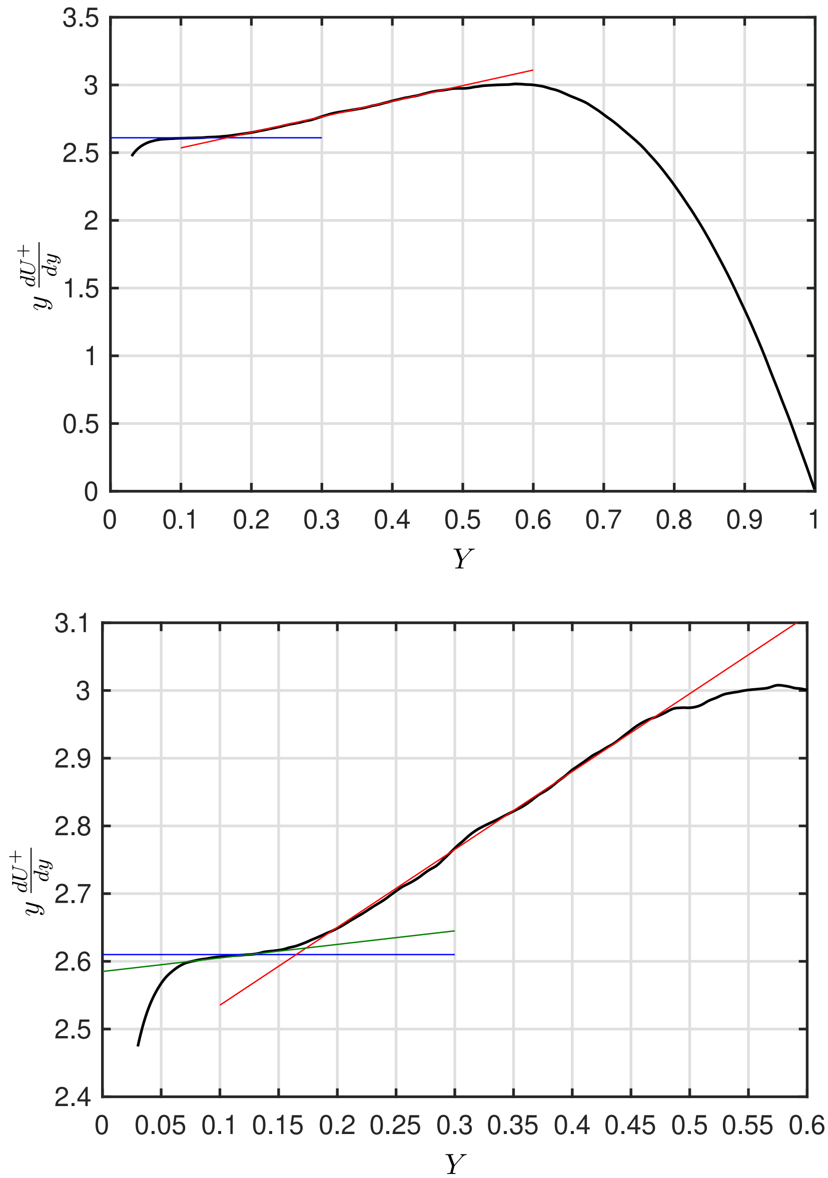

FIG. 2. Channel flow at $Re_\tau \simeq 5200$ - Function $y\,\frac{dU^+}{dy} = \frac{1}{\kappa} + Q(Y)$ up to $Y = 1$ (top) and zoom on the part up to $Y = 0.6$ (bottom): DNS[7] (black), effective $\frac{1}{\kappa} = 2.61$ used for the pseudo-plateau (blue) and line of slope $\alpha = 1.15$ (red); its intercept with the pseudo-plateau is $Y_c = 0.165$. The slight tilt [7] of the pseudo-plateau, with slope $\alpha_0 = 0.20$, is also shown (green).

at the interface separating the two, and assuming that this interface fluctuates randomly about a mean position, with a Gaussian probability distribution of mean μ and standard deviation σ, resulting in:

$$U^+ = \left(\frac{1}{\kappa}\,\ln(y^+) + C\right)\,(1-E) + U_0^+\,E \quad \text{where} \quad E(y) = \frac{1}{2}\left(1 + \operatorname{erf}\left(\frac{y-\mu}{\sqrt{2}\,\sigma}\right)\right)\,. \qquad (10)$$

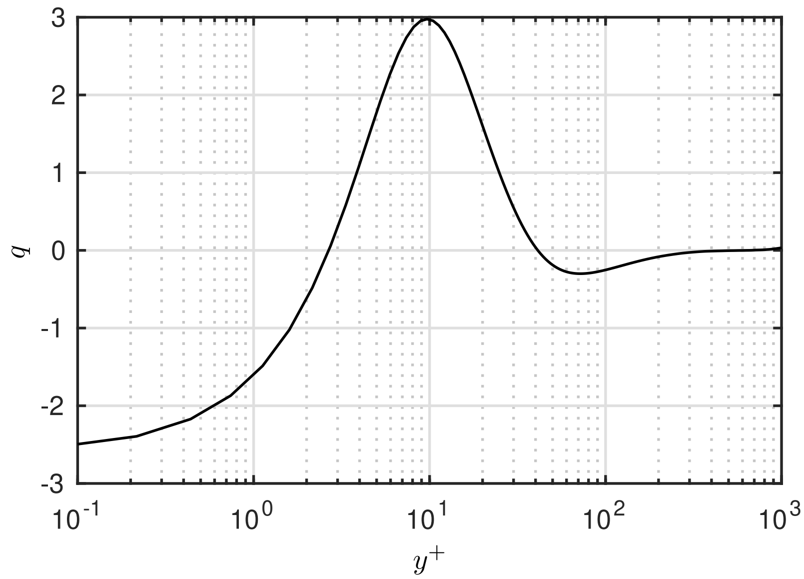

FIG. 3. Channel flow at $Re_\tau \simeq 5200$ - Inner $q(y^+)$ function from the DNS[7].

I we consider the 1% value of E (thus $(1-E) = 0.99$), this corresponds to the location $y_c \simeq \mu - 2.3\,\sigma$ as estimate for the start of the wake function. For the channel flow, they report, as best fit values to the data, $\frac{\mu}{\delta} = 0.75$ and $\frac{\sigma}{\delta} = 0.25$: the estimate is thus obtained as $Y_c \simeq 0.17$: this is very close to what we will measure in Section II. For the boundary layer, they report the lower values $\frac{\mu}{\delta} = 0.54$ and $\frac{\sigma}{\delta} = 0.19$: the estimate is thus $Y_c \simeq 0.10$: this too is very close to what we will measure in Section III.

Side note: we also notice, in Fig 1, a slight overshoot above the log law of the velocity profile. This is well recognised by now, and it is part of the argument that the beginning of the log law depends on Re_τ (a beginning at $y^+ \simeq 3\sqrt{Re_\tau}$ being reported in Marusic *et al.*[12]). This overshoot is also expected when examining the behaviour of the $q(y^+)$ function defined for the near-wall part of the indicator function as $y\,\frac{dU^+}{dy} = q(y^+) + \frac{1}{\kappa}$, see Fig. 3: it is related to the slight negative undershoot of the $q(y^+)$ profile observed before $y^+ \simeq 300$.

II. MODEL OF THE WAKE FUNCTION IN CHANNEL FLOW

We proceed with our investigation and modelling of the function $Q(Y)$; and then of the wake function $F(Y)$ obtained by its analytical integration.

Simplest model: In the simplest version, we solely consider the dominating slope, $\alpha \simeq 1.15$, but with the offset. The value of the effective plateau is then measured as $\frac{1}{\kappa} \simeq 2.61$, see Fig. 2 (in blue). As the transition to the linear behaviour of $Q(Y)$ with the large slope α is quite short, we use a simple "ramp function" model. The intercept of that ramp function is then also measured: this gives $Y_c \simeq 0.165$. The simplest model is thus taken as:

$$Q(Y) = \begin{cases} 0 & \text{for } Y \leq Y_c \\ \alpha\,(Y - Y_c) & \text{for } Y_c \leq Y \leq Y_r \ . \end{cases} \tag{11}$$

Its analytical integration provides the model for the wake function, valid up to $Y_r \simeq 0.5$:

$$F(Y) = \begin{cases} 0 & \text{for } Y \leq Y_c \\ \alpha\,\left[(Y - Y_c) - Y_c \ln\left(\frac{Y}{Y_c}\right)\right] & \text{for } Y_c \leq Y \leq Y_r \ . \end{cases} \tag{12}$$

The comparison between the model and the DNS data is shown in Fig. 4 (bottom): the fit is indeed quite good (even up to $Y \simeq 0.55$).

It is also verified that the $F(Y)$ function has a zero slope at $Y = Y_c$. The first term in the Taylor series is indeed quadratic:

$$F(Y) \simeq \alpha\, Y_c \frac{1}{2}\left(\frac{Y}{Y_c} - 1\right)^2 - \ldots \qquad \text{for} \qquad 0 \leq \frac{Y}{Y_c} - 1 \ll 1 \ . \tag{13}$$

This is as opposed to the linear $Q(Y)$ without offset, Eq. (8), which produces a $F(Y)$ that is linear relatively to $Y = 0$. We recall that Coles model for $F(Y)$ is also quadratic relatively to its origin; that model will be revisited in Section IV, and it will also be improved using the offset. Note that we could use a mollified ramp function (= integral a mollified Heaviside function) for the $Q(Y)$ model. This would however be at the expense of obtaining a more complex expression for the $F(Y)$ model, and for little added value; the fit to the DNS data being already satisfactory when using the ramp function above.

For further comparison, the "extended law of the wall" model[8] is also fitted to the data. Recall that it is proposed as being valid from the start of the overlap layer (here $Y \simeq 0.06$) up to $Y_r \simeq 0.5$. The slope they measured is also $\alpha \simeq 1.15$. The effective $\frac{1}{\kappa}$ value to use with that model is no longer the 2.61 of the pseudo-plateau that is observed in the indicator function of Fig. 2 ; it is rather the intercept between the red line (extended to the left) and the ordinate, hence 2.42. To avoid any confusion, we will write it as $\frac{1}{\kappa_e} = 2.42$ (subscript

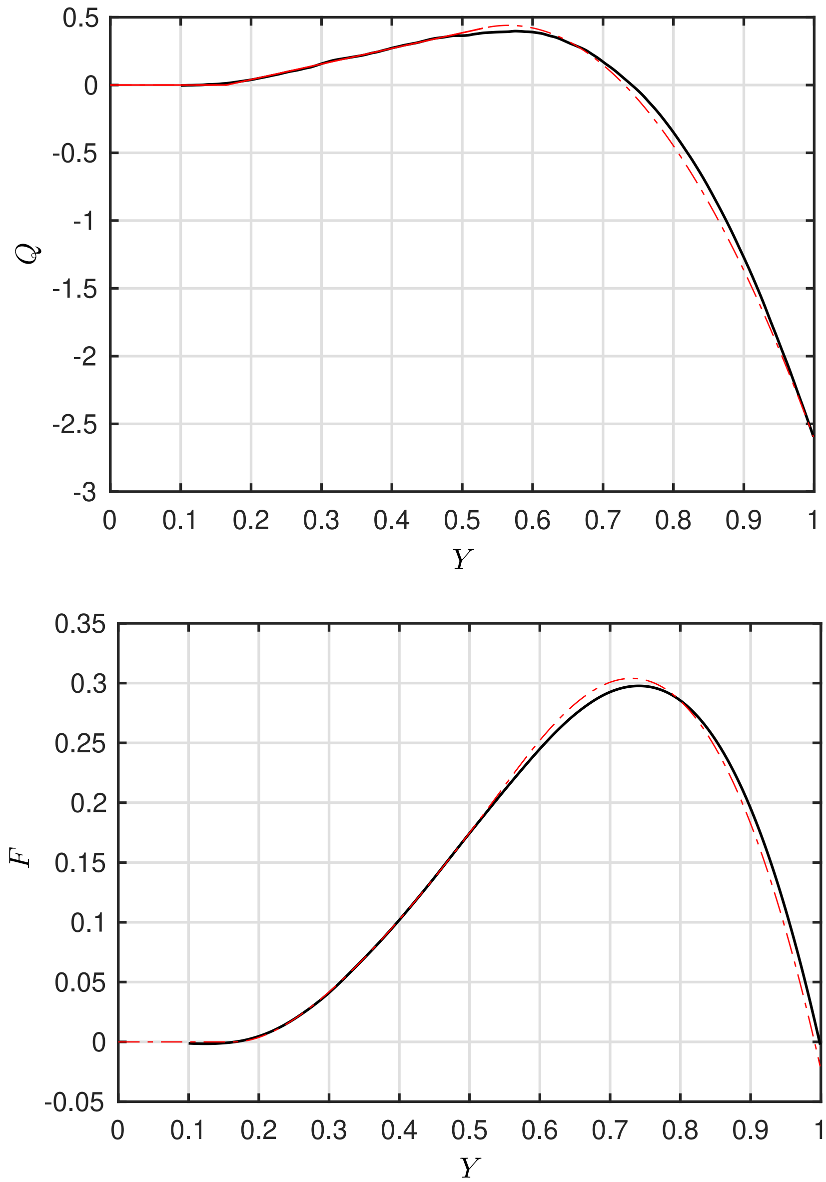

FIG. 4. Channel flow at $Re_\tau \simeq 5200$ - Function Q (top) : DNS[7] (black) and complete model: Eq. (11) (red solid) followed by Eq. (19) (red dash-dot). Wake function F (bottom): DNS[7] (black) and complete model (red dash-dot).

"e" for "extended", thus $\kappa_e \simeq 0.413$). We stress that, by construction, the two models for the indicator function $y\,\frac{dU^+}{dy}$ are identical beyond Y_c since

$$2.61 + 1.15\,(Y - 0.165) = 2.42 + 1.15\,Y \qquad \text{for} \qquad Y \geq 0.165\,. \tag{14}$$

They are however different in the range $0.06 \leq Y \leq 0.165$ that concerns the overlap layer. The C_e value to use for their model must also be adjusted so that the obtained velocity

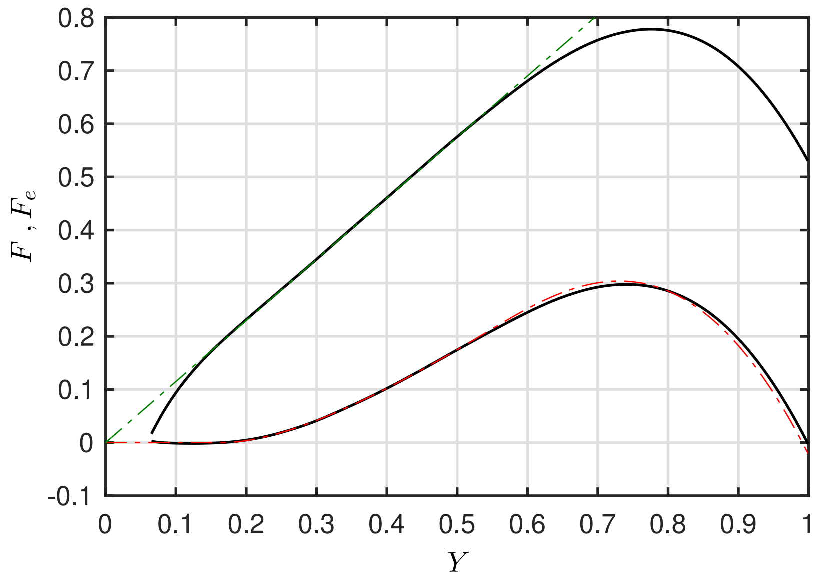

FIG. 5. Channel flow at $Re_\tau \simeq 5200$ - Functions $F(Y)$ and $F_e(Y)$: DNS[7] (black), complete model with offset for $F(Y)$ (red dash-dot), $F_e(Y) = \alpha\, Y$ of the "extended law of the wall" model[8] (green dash-dot).

profile best fits the DNS data: we obtained $C_e \simeq 5.34$. The extended law of the wall model, as calibrated on the present DNS data, finally reads

$$U^+ = \left(\frac{1}{\kappa_e}\, \ln(y^+) + C_e\right) + \alpha\, Y = \Big(2.42\, \ln(y^+) + 5.34\Big) + 1.15\, Y\ . \tag{15}$$

The exact function $F_e(Y) = U^+ - \left(\frac{1}{\kappa_e}\, \ln(y^+) + C_e\right)$ was measured using the DNS data and is presented in Fig. 5 together with the model, $F_e(Y) = 1.15\, Y$. The exact function is indeed linear in the range from 0.13 to 0.55, but this is not true in the range from 0.06 to 0.13. The extended law of the wall model is thus quite acceptable as an approximate and simple model up to $Y \simeq 0.55$, yet it does not fit well the DNS data within the overlap layer itself.

For comparison, our model for the first part up to $Y \simeq 0.55$ reads

$$U^+ = \begin{cases} (2.62\, \ln(y^+) + 4.25) & \text{for } Y \leq 0.165 \\ (2.62\, \ln(y^+) + 4.25) + 1.15\, \left[(Y - 0.165) - 0.165\, \ln\left(\frac{Y}{0.165}\right)\right] & \text{for } 0.165 \leq Y \leq 0.5\ . \end{cases} \tag{16}$$

A strict log law is preserved within the overlap layer with the slope 2.61 (thus $\kappa \simeq 0.383$) corresponding to the plateau in the measured indicator function; and the wake function $F(Y)$ only starts at $Y \simeq 0.165$.

A modified version of our model: If, following Lee and Moser[7], we wish to also include the small tilt angle, $\alpha_0 \simeq 0.2$, in the overlap layer (in green in Fig. 2), we use instead $\frac{1}{\kappa} + \alpha_0\, Y \simeq 2.59 + 0.2\, Y$ there (2.59 being the intercept between the green line and the ordinate), and we write:

$$Q(Y) = \begin{cases} \alpha_0\, Y & \text{for } Y \leq \tilde{Y}_c = \frac{\alpha}{(\alpha-\alpha_0)}\, Y_c \\ \alpha\,(Y - Y_c) & \text{for } \tilde{Y}_c \leq Y \leq Y_r\ . \end{cases} \tag{17}$$

The integration produces the corresponding $F(Y)$ model:

$$F(Y) = \begin{cases} \alpha_0\, Y & \text{for } Y \leq \tilde{Y}_c \\ \alpha_0\, \tilde{Y}_c + \alpha\, \left[(Y - \tilde{Y}_c) - Y_c\, \ln\left(\frac{Y}{\tilde{Y}_c}\right)\right] & \text{for } \tilde{Y}_c \leq Y \leq Y_r\ . \end{cases} \tag{18}$$

That model is more complex; yet the dominating ingredient remains the contribution of the large slope α with the offset Y_c. Judging from Fig. 4, our simplest model without α_0 will clearly suffice for most applications.

A complete model covering the full range: Finally, and in either case (simplest or more complex), the $Q(Y)$ model above can be further extended to cover the rest of the range, up to $Y = 1$. The easiest way is to subtract from the linear ramp function a term that is quadratic relatively to Y_r so as to satisfy the boundary condition that $Q(1) = -\frac{1}{\kappa}$:

$$Q(Y) = \alpha\,(Y - Y_c) - \beta\,(Y - Y_r)^2 \qquad \text{for} \qquad Y_r \leq Y \leq 1\ , \tag{19}$$

where β is obtained from the boundary condition:

$$\beta = \frac{\left[\frac{1}{\kappa} + \alpha\,(1 - Y_c)\right]}{(1 - Y_r)^2}\ . \tag{20}$$

The integration then leads to

$$\begin{aligned} F(Y) = F(Y_r) + \alpha\, &\left[(Y - Y_r) - Y_c\, \ln\left(\frac{Y}{Y_r}\right)\right] \\ - \beta\, &\left[\frac{1}{2}\left(Y^2 - Y_r^2\right) - 2\, Y_r\,(Y - Y_r) + Y_r^2\, \ln\left(\frac{Y}{Y_r}\right)\right] \quad \text{for } Y_r \leq Y \leq 1 \end{aligned} \tag{21}$$

where $F(Y_r)$ is given by Eq. (12) or Eq. (18), depending on the choice of model used for the first part. The Y_r value used for our complete model above can also be chosen so as to best fit globally the $Q(Y)$ function (while of course maintaining the measured slope $\alpha = 1.15$ and

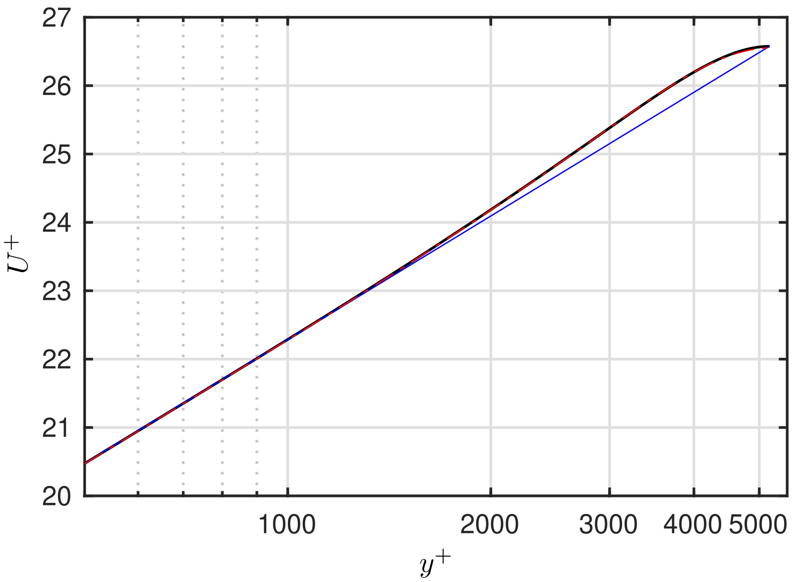

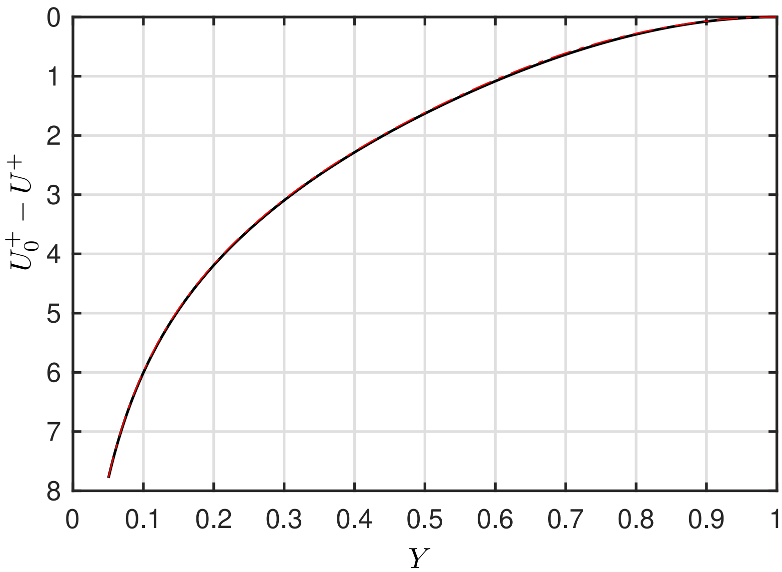

FIG. 6. Channel flow at $Re_\tau \simeq 5200$ - Velocity U^+ (top): DNS[7] (black) and complete model: Eq. (12) followed by Eq. (21) (red dash-dot). The log-law with $\kappa = 2.61$ and $C = 4.25$ is also shown (blue). Defect law $U_0^+ - U^+$ (bottom).

measured intercept $Y_c = 0.165$): we used $Y_r = 0.53$. The comparisons between our complete model (simplest version) and the DNS data are shown in Fig. 4. The modelled velocity and defect law profiles are presented in Fig. 6.

For further comparison, we also examine the DNS data of channel flow of Hoyas and Jiménez[13] at the lower $Re_\tau \simeq 2000$. We see, in Fig. 7, that the $Q(Y)$ function is similar to that measured in the DNS at $Re_\tau \simeq 5200$: same slope $\alpha \simeq 1.15$, and same shape. The Reynolds number is here too low to have a well-defined overlap layer; an estimate for the intercept, obtained using $\frac{1}{\kappa} \simeq 2.61$ from the DNS $Re_\tau \simeq 5200$, gives $Y_c \simeq 0.11$.

Proposition: A question then arises as to what happens to Y_c when the Reynolds number is increased much beyond $Re_\tau \simeq 5200$? One possibility is that it remains at essentially the same value as that measured using the DNS data at $Re_\tau \simeq 5200$ (that has a fair overlap layer); the wake function $F(Y)$ measured and modelled above is then already the asymptotic one. Another possibility is that the Y_c value still grows a little, and settles at a value a bit higher than $Y_c \simeq 0.165$ when $Re_\tau \to \infty$. Such growth must however remain quite limited: indeed, the $Q(Y)$ function that starts positive and linear must also be negative in a wide range so as to satisfy the condition that $Q(1) = -\frac{1}{\kappa}$. Our proposition is that the value $Y_c \simeq 0.165$ is already close to the asymptotic one; and hence also the wake function $F(Y)$ measured and modelled above.

III. MODEL OF THE WAKE FUNCTION IN ZPG BOUNDARY LAYER

We examine the DNS data of a zero pressure gradient (ZPG) boundary layer at $Re_\tau \simeq 2300$ of Sillero, Jiménez, and Moser[14]. We see, in Fig. 7, that $Q(Y)$ also exhibits a linear behaviour up to $Y \simeq 0.5$, but with a much larger slope than for the channel flow. We also fit the wake function using the complete model of Eq. (12) followed by Eq. (21). The "effective thickness" δ used for the model is also found as part of the fit to the DNS data: the model being used for $Y = y/\delta \leq 1$ with a zero slope at $Y = 1$, and a uniform velocity $U_0 = U_e$ being used above, where U_e is the outer flow velocity of the DNS. For further consistency, we also impose that the model profile and the DNS profile have the same $\int_{Y_c}^{\infty} (1 - U/U_0)\, dY$ (the integrand being zero above $Y = 1$ for the model). The parameters are then finally obtained as: $\delta^+ = Re_\tau \simeq 2334$, $\alpha \simeq 7.3$, $Y_c \simeq 0.11$ (intercept measured assuming again $\frac{1}{\kappa} \simeq 2.61$) and $Y_r \simeq 0.44$. The final results are then shown in Figs. 8 and 9: here too, the wake model is seen to fit very well the DNS data.

Proposition: It is possible that the intercept could be a bit above $Y_c \simeq 0.11$ for a ZPG boundary layer at $Re_\tau \simeq 5000$ (something to investigate when such DNS become available).

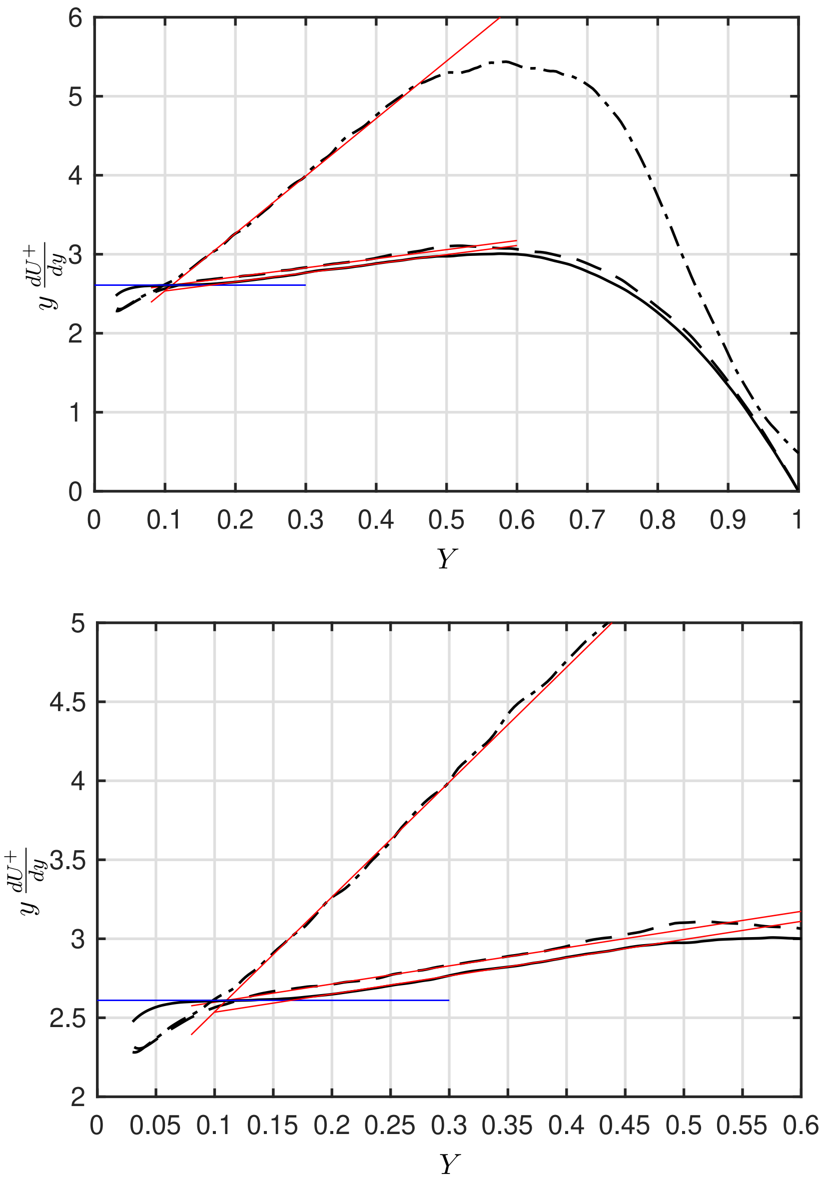

FIG. 7. Function $y\,\frac{dU^+}{dy}$ up to $Y = 1$ (top) and zoom on the part up to $Y = 0.6$ (bottom): DNS of channel flow at $Re_\tau \simeq 5200$[7] (solid) and at $Re_\tau \simeq 2000$[13] (dash); DNS of ZPG boundary layer flow at $Re_\tau \simeq 2300$[14] (dash-dot). Also shown are $\frac{1}{\kappa} \simeq 2.61$ (blue) and the lines of slope α (red).

If it does, it will nevertheless be smaller than the $Y_c \simeq 0.165$ of channel flow: indeed, since the slope α is here much larger and since $Q(Y)$ must again go negative over a wide range so as to connect to the outer flow with $Q(1) = -\frac{1}{\kappa}$, there is here less room for Y_c to increase much above $\simeq 0.11$; we refer to Fig. 7 to appreciate our proposition.

The value of the offset Y_c is clearly case-dependent. Recall that this is also confirmed

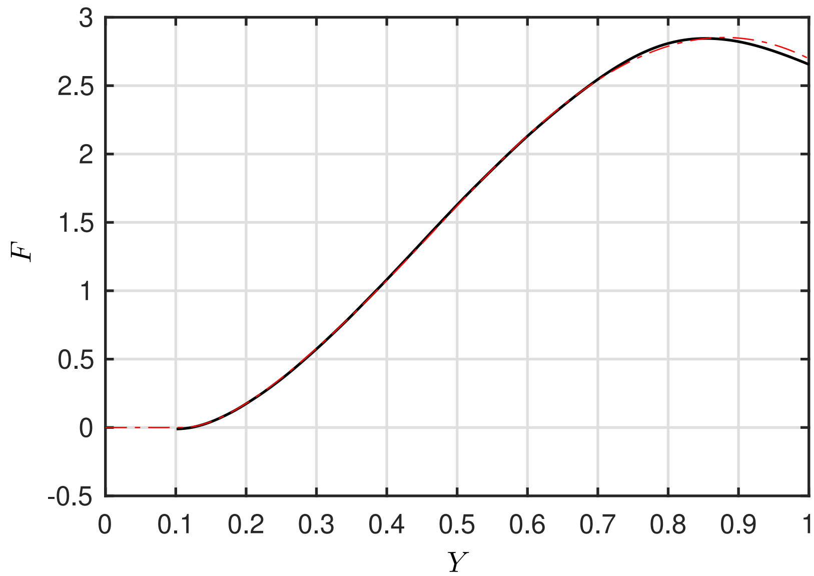

FIG. 8. ZPG boundary layer at $Re_\tau \simeq 2300$ - Wake function F : DNS[14] (black) and complete model: Eq. (12) followed by Eq. (21) (red dash-dot).

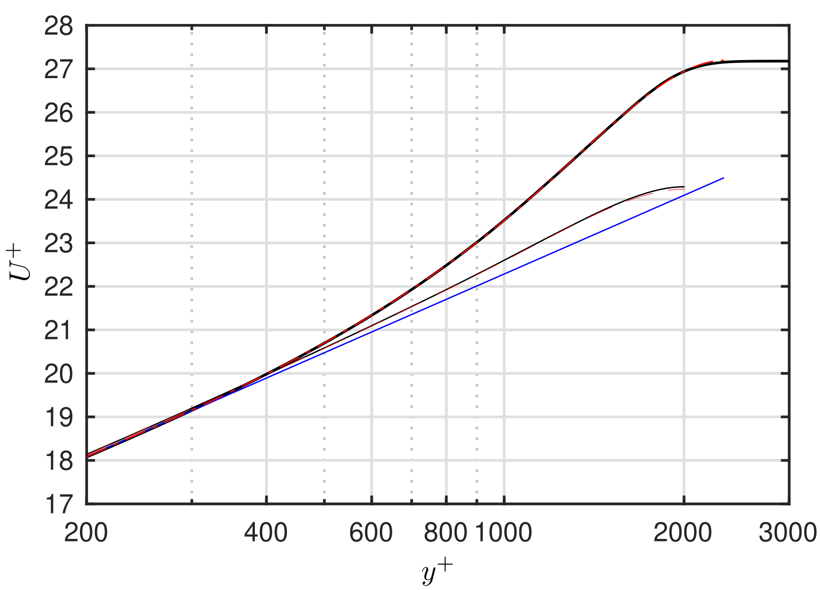

FIG. 9. ZPG boundary layer at $Re_\tau \simeq 2300$ - Velocity U^+ : DNS[14] (black) and complete model: Eq. (12) followed by Eq. (21) (red dash-dot). The channel at $Re_\tau \simeq 2000$ is also shown for comparison: DNS[13] (black) and complete model (red dash-dot). The log-law with $\kappa = 2.61$ and $C = 4.25$ is also shown (blue).

by our previous analysis of the "two state model"[11]. It actually makes sense that "the larger the amplitude of the wake function, the smaller the offset". The channel flow has a wake function with a very small amplitude (see Fig. 6) and an offset of $Y_c \simeq 0.165$; the ZPG boundary layer has a much larger wake function (see Fig. 9) and a smaller offset of $Y_c \simeq 0.11$ (possibly a bit higher when at very high Re_τ). If we further consider, as Coles did, the limiting case of an adverse pressure gradient boundary layer very close to separation, then the whole velocity profile will be "only the wake function" (in the sense that the "law of the wall" is totally overshadowed by the "law of the wake") with zero offset.

IV. IMPROVED COLES-TYPE MODELS

Coles model amounts to using:

$$F(Y) = A\,\sin^2\left(\frac{\pi}{2}\,s\right) \quad \text{or} \quad F(Y) = A\,\left(3\,s^2 - 2\,s^3\right) \quad \text{with} \quad s = \frac{Y}{Y_m} = \frac{y}{y_m} \tag{22}$$

where y_m is the location of the observed maximum of the wake function. In Coles notation, the amplitude A is written $2\,\frac{\Pi}{\kappa}$. The use of the $\sin^2$ function is the original version by Coles; the polynomial function constitutes an alternative choice often used in the literature; hence we consider both. They are much alike for $0 \leq s \leq 1$, but not beyond: the polynomial function then goes significantly below the $\sin^2$ function.

We stress that Coles only proposed his $F(Y)$ model to fit the wake function of boundary layers. We also recall that he used as boundary layer thickness the location y_m where the measured wake function is maximum. Thus, with our definition of δ, Coles model is indeed that of Eq. (22).

Using the DNS[14], the maximum of the wake function is seen to occur at $Y_m \simeq 0.85$, and with amplitude $A \simeq 2.85$: the model using those coefficients is then shown in Fig. 10 and for both versions: it does not fit well the DNS data at low Y. The model is improved when taking into account the offset; hence using instead $s = \frac{(Y-Y_c)}{(Y_m-Y_c)}$. This is shown in Fig. 10 (top) with $Y_c = 0.11$ (as used with the model of Eq. (11)). We also note that the original version does slightly better than the polynomial one beyond Y_m. The global fit can even be further improved by adjusting the offset: see bottom of Fig. 10.

We then also apply the model to the channel flow DNS[7]. The maximum of the wake function is seen to occur at $Y_m \simeq 0.74$, with $D \simeq 0.30$: the model using those coefficients

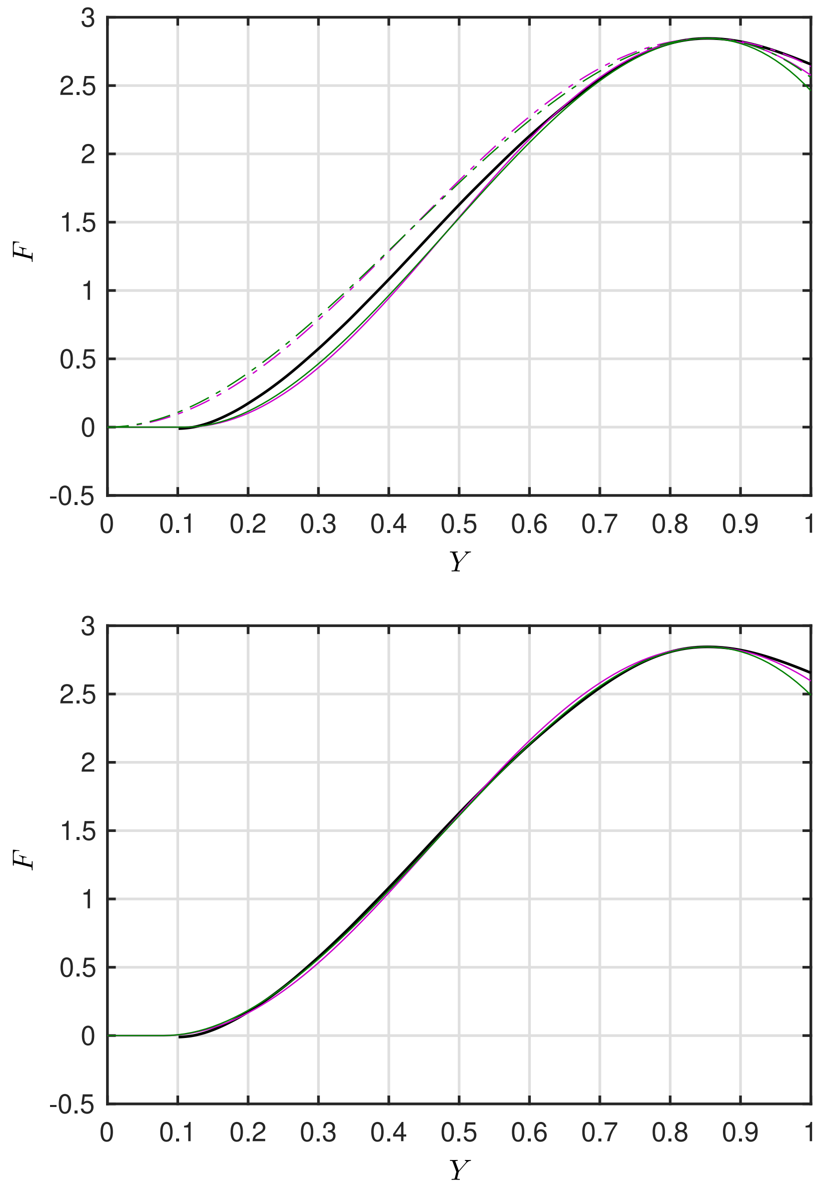

FIG. 10. ZPG boundary layer - Wake function F : DNS[14] (black); original Coles model (magenta dash-dot) and polynomial version (green dash-dot); improved models using $Y_c = 0.11$ (magenta solid and green solid) (top); improved models using $Y_c = 0.08$ (bottom).

is shown in Fig. 10, again for both versions: it constitutes a poor fit to the DNS data. The improved models are shown in Fig. 11, with $Y_c = 0.165$ (as used with the model of Eq. (11)). Here the polynomial version does significantly better than the original one beyond Y_m (its slope at $Y = 1$ is then $\simeq -2.1$; thus still not $\simeq -2.6$).

We stress again that the amplitude of the wake function in channel flow is much smaller than in the ZPG boundary layer (roughly 10 times smaller).

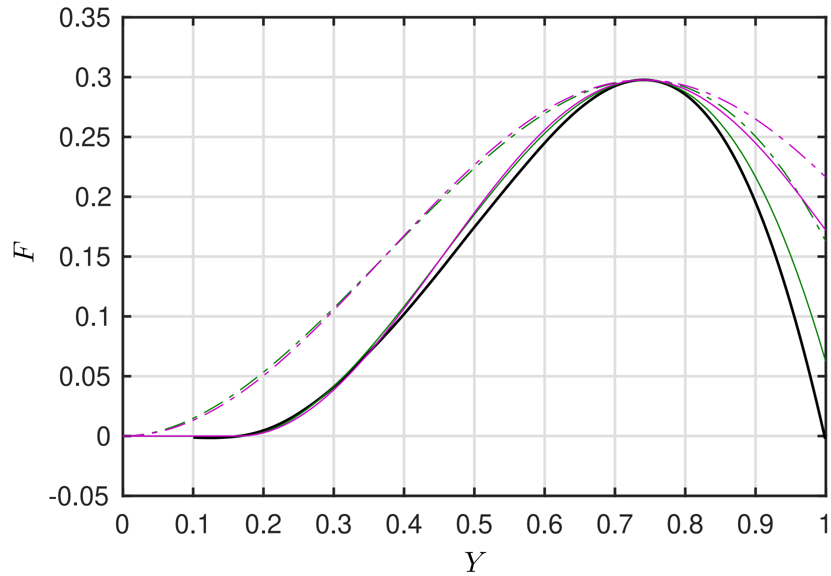

FIG. 11. Channel flow - Wake function F : DNS[7] (black); original Coles model (magenta dash-dot) and polynomial version (green dash-dot); improved models using $Y_c = 0.165$ (magenta solid and green solid).

V. CONCLUSION

We first used the data of high quality DNS of a turbulent channel flow at $Re_\tau = 5200$[7] to measure the various components of $y\,\frac{dU^+}{dy} = \frac{1}{\kappa} + Q(Y)$ for the outer region: the overlap layer and beyond. We then produced complete models for $Q(Y) = Y\,F'(Y)$; and then, by analytical integration, for the wake function $F(Y)$.

For the simplest version of the $Q(Y)$ model: the first part is linear with slope of $\alpha \simeq 1.15$, and it starts at the measured intercept $Y_c \simeq 0.165$: $Q(Y) = \alpha\,(Y - Y_c)$. This linear behaviour is seen to be valid up to $Y_r \simeq 0.5$. The model was then also further extended up to the channel centre ($Y = 1$) by subtracting a term that is quadratic relatively to Y_r so as to satisfy the boundary condition that $Q(1) = -\frac{1}{\kappa}$. The integration of the $Q(Y)$ model then provided a complete model for the $F(Y)$ wake function, and which is seen to reproduce very well that measured in the DNS, over the full range.

Our model with offset was also usefully compared, in its first part, to the "extended law of the wall" model[8] as fitted to the present DNS data.

We also provided how our model can be further modified if one wishes to stick with the view that $Q(Y)$ is not strictly zero in the overlap layer but rather has a small linear slope there (i.e., $Q(Y) = \alpha_0 Y$ there; yet with $\alpha_0 \ll \alpha$): it suffices to add this small contribution before the most important and dominating part, $\alpha\,(Y - Y_c)$. As our focus is not the discussion on whether or not there a strict law of the wall, but rather on producing a reasonably accurate model for the wake function, our view is that adding a small $\alpha_0 Y$ contribution is not necessary; nor useful.

Our model was then also applied to the ZPG boundary layer, using DNS data at $Re_\tau \simeq 2300$[14]: the amplitude of the wake function is much larger than in channel flow (roughly 10 times larger), and the measured slope and intercept are $\alpha \simeq 7.3$ and $Y_c \simeq 0.11$ (Y_c possibly a bit higher when at very high Re_τ). Our complete model for the wake function was also found to reproduce very well that measured in the DNS.

Clearly, the value of the offset Y_c is case-dependent; as also confirmed by the "two state model"[11] fitted on channel flow and ZPG boundary layer. It actually makes sense that "the larger the amplitude of the wake function, the smaller the offset": since $Q(Y)$ that starts positive in its first part with the slope α must also go negative over a wide range so as to satisfy the boundary condition that $Q(1) = -\frac{1}{\kappa}$, a relatively larger slope α in its first part is naturally associated with a relatively smaller offset.

Finally, a simple "Coles-type model" was also offered and tested: it amounts to modify the wake function model of Coles by taking the Y_c offset into account; which significantly improves the fit to the DNS data.

ACKNOWLEDGMENTS

The interest of the main author in wall-bounded turbulence started with the lectures from Donald Coles that he followed when studying at Caltech. He is also grateful to Anthony Leonard for the fruitful discussions, over many years, about our investigations of the laws of the wall and of the wake using DNS data of constantly increasing Reynolds number and quality. He also thanks Beverly McKeon for a fruitful discussion about some of the work reported here. The authors also benefited from previous investigations of DNS data done in close collaboration with Laurent Bricteux.

REFERENCES

[1]T. Von Karman, "Mechanische ahnlichkeit und turbulenz," Nachr. Ges. Wiss. Gottingen, Math-Phys. Klasse (1930).

[2]L. Prandtl, "7. bericht über untersuchungen zur ausgebildeten turbulenz," ZAMM-Journal of Applied Mathematics and Mechanics/Zeitschrift für Angewandte Mathematik und Mechanik **5**, 136–139 (1925).

[3]C. B. Millikan, "A critical discussion of turbulent flow in channels and circular tubes," in *Proc. 5th Int. Congress on Applied Mechanics (Cambridge, MA, 1938)* (Wiley, 1938) pp. 386–392.

[4]D. Coles, "The law of the wake in the turbulent boundary layer," Journal of Fluid Mechanics **1**, 191–226 (1956).

[5]N. Afzal and K. Yajnik, "Analysis of turbulent pipe and channel flows at moderately large Reynolds number," Journal of Fluid Mechanics **61**, 23–31 (1973).

[6]J. Jiménez and R. D. Moser, "What are we learning from simulating wall turbulence?" Philosophical Transactions of the Royal Society A: Mathematical, Physical and Engineering Sciences **365**, 715–732 (2007).

[7]M. Lee and R. D. Moser, "Direct numerical simulation of turbulent channel flow up to $Re_\tau \approx 5200$," Journal of Fluid Mechanics **774**, 395–415 (2015).

[8]M. Bernardini, S. Pirozzoli, and P. Orlandi, "Velocity statistics in turbulent channel flow up to $Re_\tau = 4000$," Journal of Fluid Mechanics **742**, 171–191 (2014).

[9]P. Luchini, "Universality of the turbulent velocity profile," Physical review letters **118**, 224501 (2017).

[10]P. Luchini, "Structure and interpolation of the turbulent velocity profile in parallel flow," European Journal of Mechanics-B/Fluids **71**, 15–34 (2018).

[11]D. Krug, J. Philip, and I. Marusic, "Revisiting the law of the wake in wall turbulence," Journal of Fluid Mechanics **811**, 421–435 (2017).

[12]I. Marusic, J. P. Monty, M. Hultmark, and A. J. Smits, "On the logarithmic region in wall turbulence," Journal of Fluid Mechanics **716** (2013).

[13]S. Hoyas and J. Jiménez, "Scaling of the velocity fluctuations in turbulent channels up to $Re_\tau = 2003$," Physics of fluids **18**, 011702 (2006).

[14]J. A. Sillero, J. Jiménez, and R. D. Moser, "One-point statistics for turbulent wall-bounded

flows at Reynolds numbers up to $\delta^+ \approx 2000$," Physics of Fluids **25**, 105102 (2013).